MANSOURA JOURNAL OF Geology
Official Journal of Faculty of Science, Mansoura University, Egypt
E-mail: scimag@mans.edu.eg ISSN: 2974-4962

Integration of Airborne Magnetic Data and Remote sensing Technique for Geological Structural Lineaments Extraction, Gabal El-Syibaì Area, Central Eastern Desert, Egypt

Mohamed Rashwan[1*], Mohamed A.S Youssef[2], Mohamed Elsadek M. Sabra[3], Lamees Mohamed[1], Adel Kamel Mohamed[1]

[1]*Geology Department, Faculty of Science, Mansoura University, Egypt*

[2]*Nuclear Material Authority, Exploration Division, Po. Box 530, Maddi, Cairo, Egypt*

[3]*Egyptian Mineral Resources Authority, Po. Box 11517, Abbassiya, Cairo, Egypt*

**** Correspondence to:*** *m.rashwan89@std.mans.edu.eg, 01008380626*)

Received:30/9/2023
Accepted: 11/11/2023

Abstract : The study area is characterized by its geological and topographical features in terms of high terrain and steep slopes. Thus, detecting structural lineaments in these areas is critically important on the geohazard side. The current study focused on mapping the geological structural lineaments affecting the Gabal El-Syibaì area based on airborne magnetic measurements and remote sensing technique (RS). In the process of tracing structural lineaments, shaded image with a spatial resolution of 30 m derived SRTM DEM and 12.5 m shaded image derived PALSAR DEM are traced the surface lineaments. In this regard, regional and residual magnetic component, and tilt derivative methods are help in extracting the sub surface structure elements. Three trends—the NE-SW (Gulf of Aqaba trend), the N-S (East African trend), and the NNW-SSE (Gulf of Suez trend)—affected the study region at both deeper and shallower depths. The findings showed that there is an important relationship between magnetic measurements and remote sensing data when extracting structure elements. Whereas, the surface structure in the research region reflect the presence of subsurface features. So, it's important to utilise remote sensing measurements to make an initial decision before performing field investigations. These trends can be used for environmental and geohazard managements of the study area.

keywords: Gabal El-Syibaì, Lineaments, Aeromagnetic, DEM

1.Introduction

In geology, the term "lineament" is frequently used to refer to linear topographical characteristics that represent weak zones [1]. The lineament is the outcome of fractures in the Earth's crust and can take the form of faults, joints, or other linear structures. According to several studies (Milbury et al., 2007; Austin and Blenkinsop, 2008) [2,3], regional lineaments are typically understood as geologic weak zones. From geohazard point of view, the occurrence of rockfall is significantly influenced by lineaments, which are surface features but also represent underlying conditions [4]. Faults are one of the key elements influencing the possibility for landslides [5,6]. In fractured rocks, faults produce steep slopes and shear zones, increasing the likelihood of landslides [7]. Additionally, from mining point of view, lineaments are a crucial topographic feature for resource exploration for hydrocarbons, minerals, groundwater, and geothermal energy [8-13]. The Central Eastern Desert, which includes the study area, is characterized by the presence of many important economic materials, such as gold, iron, copper, and lead [1]. So, it’s important to traced the lineament of the study area for mining purpose.

In this regard, many development projects are only interested in studying surface phenomena such as geomorphology and hydrology, and neglect the subsurface investigation, which may cause sudden risks or

loss of a natural resource such as minerals. So, studying what exists below the surface is important for long-term development in order to benefit from natural resources and avoid geohazards. Magnetic survey is considered an effective tool for this purpose. Additionally, combining magnetic analysis with other information from geology and remote sensing considered an efficient approach for assessing the environmental impact of the area. Accordingly, this investigation aims to identify probable structural lineament trends of the area under investigation based on RS and airborne magnetic measurements.

The study area is located at central part of the Eastern Desert. It covers an area about 2854.8 km^2, and it bounded by longitudes 33^o 50′ 08.472″ and 34o 38′ 44.652″ East, and latitudes 25^o 32′ 23.207″ and 25^o 54′ 42.406″ North. The Red Sea Coastal Road, which borders the study area on the east, and Marsa Alam International Airport in the SE corner of the region, are convenient ways to reach the study area site (Fig.1).

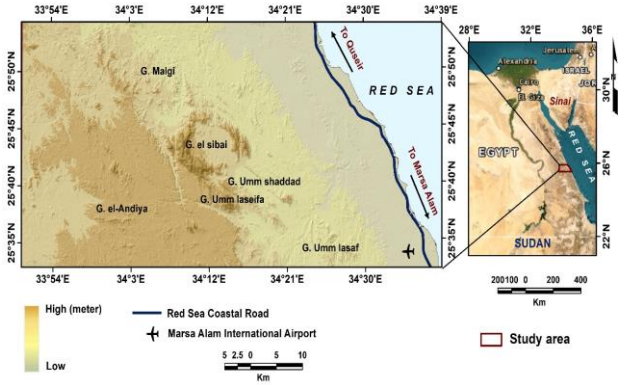

Figure 1: Location of the research region

High terrain and steep slopes are characteristics of the research area (Fig. 2a&b). The terrain elevation in the study area reaches 1452 m and is affected by slope reaches >30º. This indicates the importance of studying structural lineaments. As high elevations and extreme inclinations are among the most important factors causing an environmental hazard such as landslides. Figure 2c shows the selective location of landslides that were tracked during the field examination.

Geologically, the research region has drawn the attention of numerous geologists because it exhibits the majority of geological and structural features of the Precambrian rock units that cover Central Eastern Desert [15]. Two main rock units cover the study area; Pre-Cambrian igneous and metamorphic rock units and Sedimentary units. In terms of sedimentary units, the sedimentary geological units consist of rocks of the Cretaceous, Tertiary, and Quaternary period, which cover the Red Sea coast and some location over the area. It also forms the deposits of wadis that cross the research region to East as well as West direction. Additionally, the basement rocks, which are igneous and metamorphic rocks, are crystalline in nature and free from fossils. Latest works in the Eastern Desert shows that plate tectonic theories provide a more accurate explanation for how this complex evolved [16]. One of the evidences for this theory is the widespread presence of ophiolite melanges and ophiolitic sequences in the Eastern Desert, which are linked to vast metasediments with an oceanic character. Consequently, a number of plate tectonic hypotheses were put out to explain how these rocks evolved [17-19]. The geologic map [15] shows the various rock units that make up the study region as well as structural affecting the study area (Fig. 3a&b).

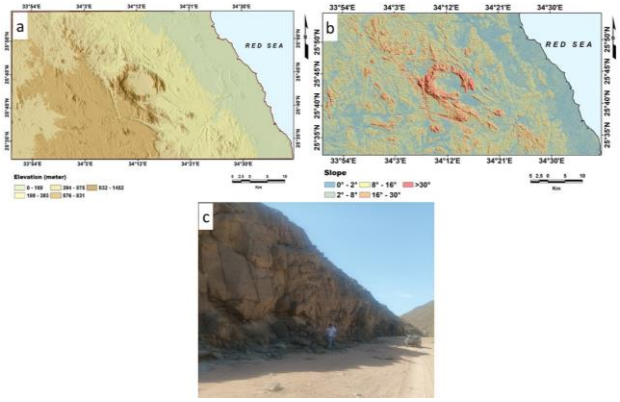

Figure 2: a) Elevation map, b) map of the slope, and c) Selective location of landslide traced in the study area through the field chick.

In terms of structure lineaments, the region witnessed a deformation event that affected the rock units during the Pan African period. The Planer and linear structural features like faults, folds, unconformities, and disconformities reflect structural deformations of the study area. These structural features control the formation of the valleys of the study area, which differ in their shapes and hydromorphometric characteristics. The research region contains a number of different types of unconformity; 1)

Non-conformity type which separates between the sedimentary rocks and basement rocks units. 2) Disconformity type between Eocene and Oligocene rock units, Ranga Formation and older sediments of Oligocene sediments, Umm Mahara Formation and Ranga Formation and between Miocene rocks and Quaternary deposits [15]. In the gable el sbai area, three foliations surfaces (S1, S2, and S3) have been identified; the S3 foliations is the most prevalent and is simpler to locate in outcrops [20]. According to Fowler et al. (2007) [21], pencil structure is widespread throughout the Central Eastern Desert, including the El Sibai region. The fine-grained metagrywakes of ophiolitic mélange matrix and siltstones of the Hammamat series, trending N30 -50 W subparallel to the major and minor fold axes in the region, are where the Pencil structure are best developed [20]. In this regard, the study area is cut by different sets of faults occurred during geologic history of the study area (Fig. 3b). The faults affecting the study area have NW-SE trend and dipping to NE and/or SW direction [20]. The El Sibai area contains an impressive system of strike-slip faults, with the best-known example being the Wadi El Shush [21]. Strike-slip faults have NW-SE trend but abruptly change strike near large bodies of hard rocks such as granitic plutons (El Sibai-Abu El Tiyur and Um luseifa plutons), then the thrust faults and related minor fold well-developed [22].

2. Materials and methods

Auto detect the structural lineaments based on remote sensing and airborne magnetic measurements mainly reflects the research methodology (Fig. 4).

The 1:500,000 geological map [15] was used as support throughout the analysis. The U.S. Geological Survey (USGS) has allowed Digital Elevation Model (DEM) for downloading. This model has measurements with 30-m spatial resolution. The DEM is derived from the Shuttle Radar Topography Mission (SRTM). In comparison to DEM obtained from optical ASTER, SRTM DEM is accurate horizontally and vertically and is less affected by weather [23,24]. SRTM DEM typically includes a lot of missing data, which are regarded illogical or anomaly areas. This anomaly was fixed and filled within ArcGIS environment using the sink and fill tools to reduce errors. After that, the projection tool is used to convert the DEM from geographic coordinates system to metric coordinates system. It's important to obtain exact measurements of the slope and other linear or areal measurements.

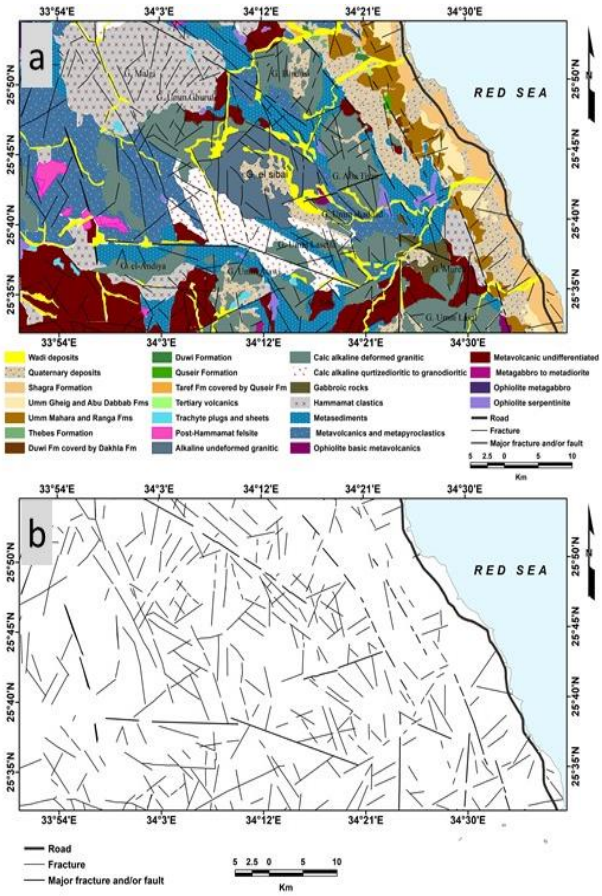

Figure 3: a) Geology of the research region after Conoco (1987), b) Geological structures derived from the geological map

In this regard, the lineaments were deduced also using Phased Array type L-band Synthetic Aperture Radar (PALSAR). PALSAR has a distinctive radar wavelength (23.62 cm with 1.27 GHz). PALSAR measurements is collected through a variety of observation modes with varying polarization, resolution, swath width, and off-nadir angle (https://asf.alaska.edu/data-sets/sar-data-sets/alos-palsar/alos-palsar-about/). PALSAR was one of three instruments aboard the Advanced Land Observing Satellite (ALOS). ALOS PALSAR helps in land-cover observation and field mapping. The NASA-sponsored ASF DAAC has allowed ALOS PALSAR data for downloading. This model has

measurements with 12.5-m spatial resolution. The SAR measurements, which have a longer wavelength and can penetrate the subsurface, are more beneficial than optical measurements in locating subsurface elements [25].

Aeromagnetic survey was carried out in Egypt in 1984 by the Division of Aero Service of the American Western Geophysical Company. This project, known as Minerals, Petroleum and Groundwater Assessment Program (MPGAP), primarily aimed to provide measurements that helps in identify mineral, petroleum, and groundwater resources [26]. In this context, the flight path should be oriented in direction perpendicular to the expected geological strike or tectonic trends of the investigation area. In this project, the spacing of flight line was close to 1.5 km and tie lines spacing of 10 km approximately. The aeromagnetic measurements were conducted at a nominal flight altitude of 120 metres (terrain clearance), with an azimuth direction of 45^{o} and 225^{o} from the true north, an inclination angle 32.8^{o} North, and a declination angle 1.9^{o} East. An airborne magnetometer known as a Varian V-85 proton free-precession magnetometer used for the investigation. Its sensitivity is 0.1 nT. Two sheets with a scale of 1:50,000 were compiled to construct the total intensity aeromagnetic map for the Gabal El Sebai region. Then these data were digitized to form a grid in order to processing and interpretation achievement. These magnetic anomalies contain some distortions regarding their location, size, and shape, resulting from the Earth's magnetic field's inclination. The magnetic measurements were improved and processed in order to adjust for these distortions and place the magnetic anomalies exactly over their actual sources. In this regard, the main objective of processing airborne magnetic measurements is to remove errors that were registered during data acquisition and extract the measured data in the form of a map for ease interpretation.

In this regard, structural lineaments of the study area are traced and autodetect through remotes sensing satellite images data covered the study area and airborne magnetic measurements. The outcome trends affecting the study area are interpreted and integrated for mining and environmental purpose.

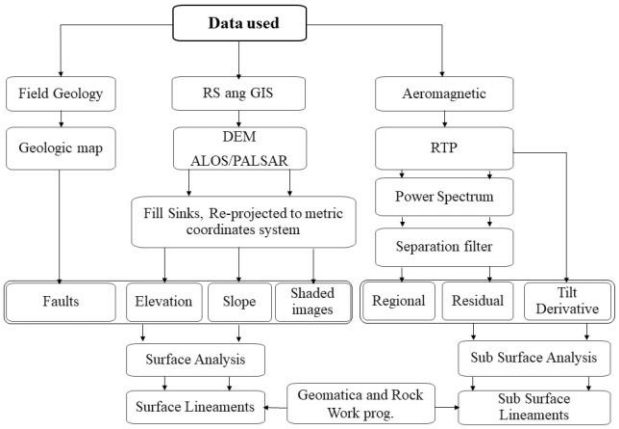

Figure 4. Flow chart outlining the study's methodology.

3. Discussion and Results

3.1. Remote sensing measurements

Shaded images are generated within the ArcGIS environment based on various sun angle directions. This type of images describes the surface phenomena in terms of sunlight falling on it. According to Jordan et al. (2005) [27], the shaded relief image is one of the best terrain models for assessing complicated hydrogeomorphological characteristics including watershed system, surface faults and fractures. The gray level within the pixels of the shaded relief image is directly proportional to the deviation angle from the normal incident of light coming from the sun. The slope that is facing the sun light will appear as a bright color while the slopes in the direction opposite to the sun light will appear as a darks color. Hence, when the sun's angle is more deviated, the gray level is higher until up to the level 256.

During the analysis, four direction filters 0º, 45°, 90º, and 135° were applied to improve the radar model. The shaded images were blend using the weighted sum tool in the ArcGIS environment. In the process of tracing structural lineaments, this property qualifies the DEM-derived shaded relief images. Figure 5a&b, show a shaded image with a spatial resolution of 30 m derived SRTM DEM and 12.5 m shaded image derived PALSAR DEM.

Automated lineament extraction was performed using algorithms and computer software [28]. To automatically extract lineaments from remotely sensed data, one of the most popular pieces of software is PCI Geomatica [29]. Automatic lineament extraction

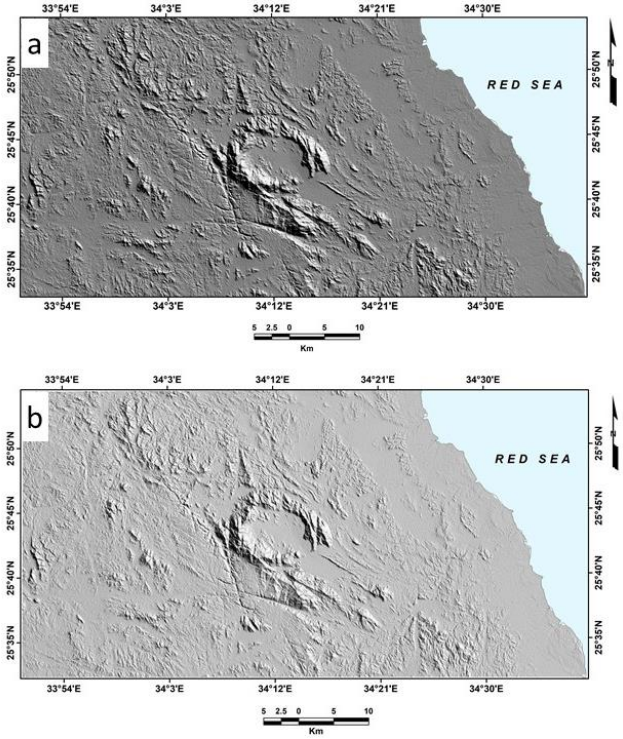

Figure 5: a) Combined shaded image with 30 m spatial resolution, b) Combined shaded image with 12.5 m spatial resolution

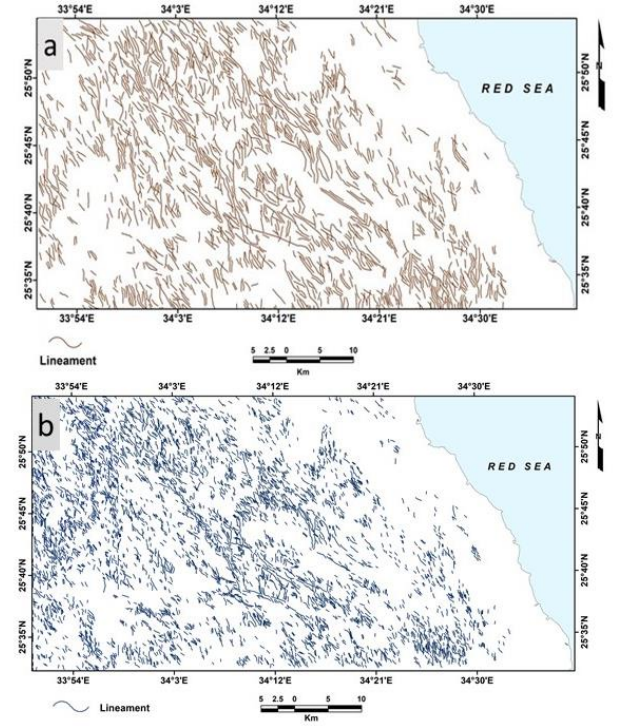

Figure 6: Lineaments map traced from a) SRTM DEM and b) PALSAR DEM

from the shaded images were carried out in the study area using PCI Geomatica program [30]. This software helps in producing vector segments that reflect linear characteristics. In this regard, there are two primary processing processes used for automatic lineaments extraction. As described by Abdullah et al. (2013) [31], the first procedure is to identify edges, which represent locations where nearby pixel values change abruptly, and the next procedure is to detect the lines. Lineaments derived from SRTM DEM and PALSAR DEM are displayed in figure 6 a&b. The orientations of the lineaments are a reflection of the tectonic events that built them.

3.2. Aeromagnetic measurements

3.2.1. Rduction to the north magnetic Pole (RTP)

In aeromagnetic surveys, this technique represents a key processing step, and forms the basis for the interpretation of magnetic anomalies [32]. A majority magnetic anomaly exhibits positive as well as negative values as a result of the earth's magnetic field's tilt. The term "reduction to the pole" refers to the transformation of measurements taken under the influence of Earth's tilted magnetic field to what they would have appeared to be if the field is perpendicular. Thus, the measurements are freed from the influence the tilting of the Earth's magnetic field. The measurements give an appearance that they were taken close to the pole, and the dipolar anomaly in this regard (the magnetic field being vertical) becomes a monopolar. In summary, after applying the RTP method (Fig. 7); 1) the reduced anomaly becomes symmetric and centered over the causing source; 2) the width of anomaly corresponds to the depth of the causative source more directly; If the body is close to the ground's surface, the anomaly has sharper shape, thus if the source is distant from the Earth's surface, the anomaly is wider; and 3) a simpler interpretation process [33].

By applying RTP filtering on the total magnetic intensity (TMI) data of the current study, the corrected map shows that the centers of the magnetic anomalies are shifted northward. Comparison of the produced RTP map, given in figure 8b with the original TMI map, illustrated in figure 8a, demonstrates this. RTP map (Fig. 6b) reveals a positive anomaly with values ranging from 0 nT to more than 354.9 nT, represented by dark yellow, red, and magenta colours. This anomaly can be traced in in the central, southern eastern, and western portions of the research region. On the other

side, there is also a negative anomaly in the southern, north eastern, and north portions of the research region, with values ranging 0 nT to less than -171 nT, and represented by yellow, green, and blue colours. To simplify analyze the data quantitatively, numerous procedures are implemented on RTP magnetic map as given below.

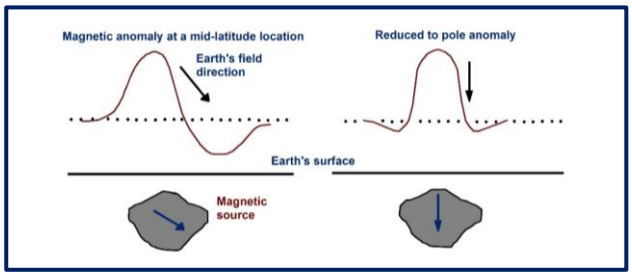

Figure 7: Illustrates how the anomaly is affected by the RTP method after Ravat (2007).

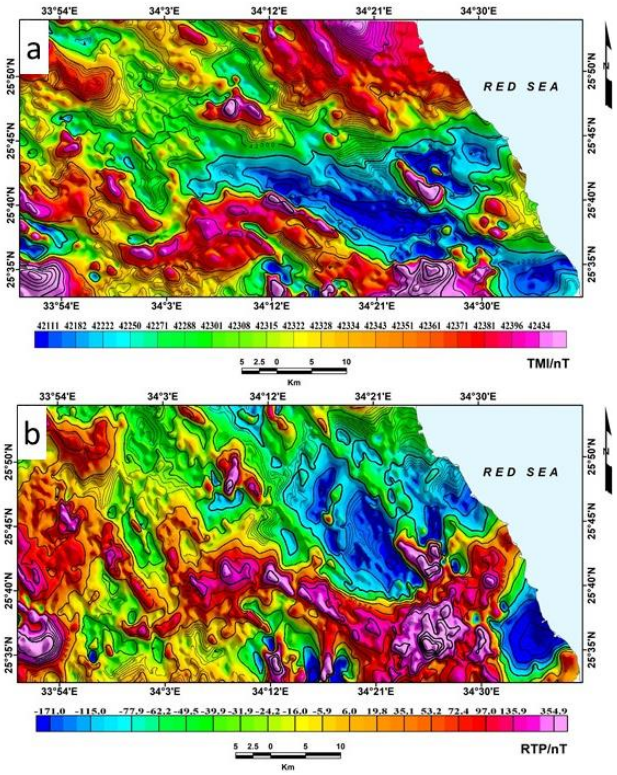

Figure 8: a) Illustrates the magnetic measurements, and b) the RTP technique

3.2.2. Power Spectrum Curve (Spectral Analysis) technique

Depending on the RTP map, separating magnetic components (regional and residual) can be done using a variety of techniques. In this regard, the deeper anomaly separates from the shallower one. One of these techniques, called Power Spectrum Curve is theoretically based on a fast Fourier Transform (FFT) [34]. Therefore, the main objective of applying spectral analysis techniques to magnetic data is to determine the mean depths of the magnetic bodies (residual or shallow) and (regional or deep). Additionally, the depth measured from Fourier spectra is the main theoretical task of the power spectrum, which has been explained by numerous researchers including Bhattacharyya (1965); Hahn et al. (1976)36; Spector and Grant (1985) [35,36,34]. According to Abdallatif and Lee (2001); Al-Badani, and Al-Wathaf (2018) [37,38]. the slope with the best linear fit is used to measure the depth. In this context, the slope of the high-frequency section is used to measure the minimum depth, whereas the slope of the low-frequency segment measures the maximum depth. Through the current study, the estimated power spectrum curve could be divided into three sections (Fig. 9). The first component, referred to as the deep causative bodies, stands for the long wavelengths. The second, also known as shallow sources, is representative of the short wavelengths. The third displays the noise component. Consequently, by measuring the slope of lines that are fitted to the upper and middle segments of the spectrum curve, respectively, it is possible to estimate the average depths of the magnetic sources (regional and residual). Results show that the deep and shallow sources had measured average depths of 1100 m and 400 m, respectively.

3.2.3. Magnetic maps (regional and residual)

Anomaly separation is a general term referring to the various processing techniques to separate the effects of shallow subsurface sources from deep ones. In this study, the filters used can be classified into two categories (High-pass and Low-pass) filters. These filters are named based on their cutoff wavelengths to "regional and residual" filters. The terms "regional and residual" filters correspond to the terms low-pass (frequency) and high pass (frequency) filters. The objective of this filter is to separate anomalies of different sizes from each other; anomalies patterns and other features can be better identified and highlighted, leading to better understanding of the geological configuration of the basement complex and the overlying sedimentary cover [39,40]. According to Reford and Sumner (1964) [41], the high-pass filter draws attention

to weaker characteristics in the magnetic map that are hidden by strong regional impacts.

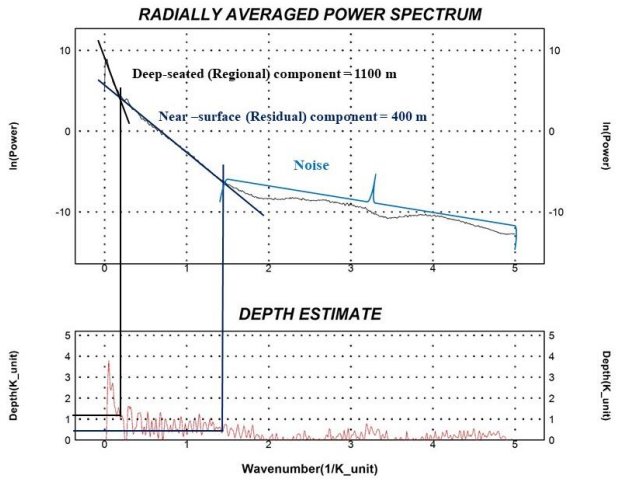

Figure 9: Power Spectrum Curve of the obtained RTP map.

a) Regional magnetic map

This regional RTP magnetic map (Fig. 10a) displays positive and negative magnetic anomalies seen all throughout the research region. The negative anomalies illustrated by the colours yellow, green, and blue, and they vary from 0 to less than -170 nT. The positive anomalies vary from 0 to more than 352 nT and are represented by the colours magenta, red, and orange. Using this map, the main trends of the research region affecting the deep-seated structures can be used to reveal.

b) Residual magnetic map

Figure 10b shows the residual RTP magnetic measurements and illustrates that the magnetic relief associated with shallow geological features and/or bodies changes sharply. This map has magnetic anomalies (positive and negative) of varying amplitude and frequency because the depths and/or compositions of the underlying sources varies. Dark yellow, magenta, red, and orange colours, with a range of 0 to more than 155 nT, are used to show positive anomalies. The negative anomalies illustrated by the colours yellow, green and blue colors, and they vary from 0 to more than -138 nT. This map can be used to show the main trends in the research region that have an impact on shallow structure lineaments.

To highlight the structure lineaments (deep and shallow) impacting the research region, structural lineaments were traced over the RTP map and its components (regional and residual) RTP magnetic map (Figs 11a&b). These maps display a significant structural framework that reflects the tectonic development.

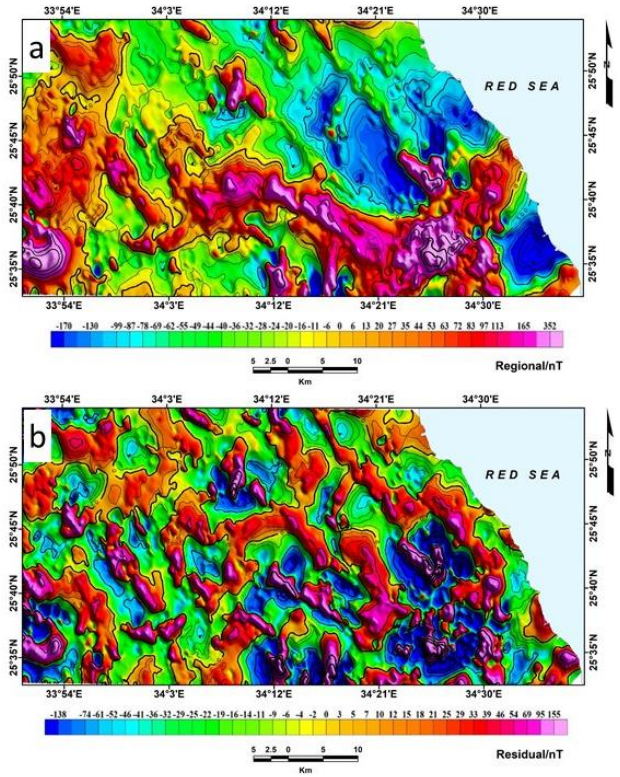

Figure 10: a) RTP regional magnetic component, b) RTP residual magnetic component of the research region.

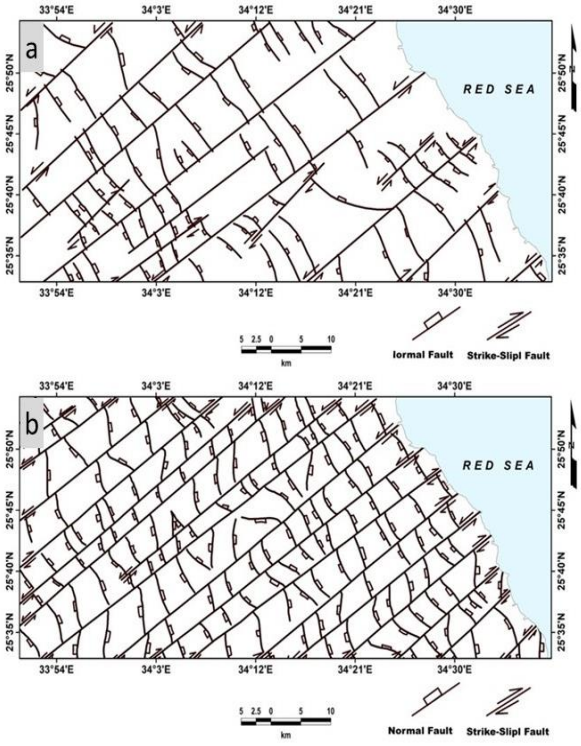

Figure 11: Interpreted structural map based on a) reginal magnetic component and b) residual magnetic component

3.2.4. Vertical Derivative

Vertical Derivative processing aims to simplify the interpretation of RTP magnetic data (Fig.12 a&b). It is the basis of the derivative application that removes low frequencies as well as addresses the impacts of nearby anomalies [42]. In this regard, to improve the shallow geologic source, the vertical derivative is frequently applied to RTP map. The boundaries of magnetic bodies are defined by the first or second vertical derivative, which highlight sources at shallow depths and indicate gradients around the edges of this sources [43,44]. In one word, to enhance the shallowest geological sources, the vertical derivative process is performed to the magnetic measurements. In this context, first vertical derivative map, which has become necessity for magnetic interpretation, is often used to reveal geologic edges and boundaries in data [45].

3.2.5. Tilt derivative (TDR)

The edges of the magnetic sources are located using a method called tilt angle derivative. TDR is a powerful technique for tracing the edges of bodies since it is highly sensitive to magnetic source boundaries. Miller and Singh (1994) [46] first proposed TDR, which was later developed by others like Verduzco et al. (2004); Salem et al. (2008) [47]. According to Miller and Singh (1994) [46], the TDR value is positive above the sources and negative when distanced from the sources, while zero values are located above or close to the boundaries of the causative bodies. In Figure 12c, the magnetic sources' edges for the current study are illustrated. In this context, the yellow line marks the borders of the magnetic bodies. According to the current analysis, the TDR map's zero contour line (yellow line) marks the location where magnetic susceptibilities between negative and positive anomalies abruptly change. Thus, the zero-contour line represents the boundaries of magnetic bodies. In the colour scale bar, you can see the yellow zero contours that separate the colours red (which have positive values) and green (which have negative values). To highlight the structural impacting the research region, structural lineaments were traced over the TDR map (Fig. 13). These maps display edges of contact and clear boundaries between structure units that reflects the tectonic development of the study area.

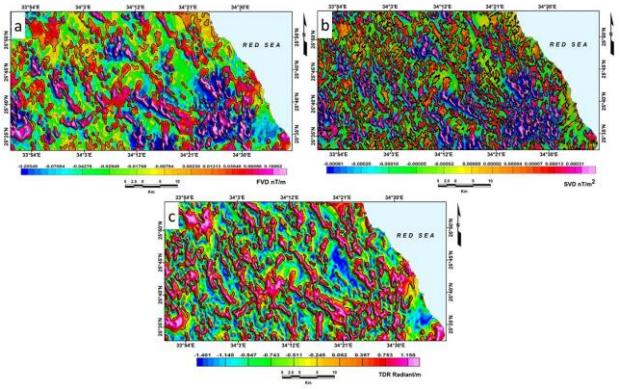

Figure 12: a) FVD, First vertical derivative b) SVD, Second vertical derivative map, c) TDR, Tilt Derivative map with boundary of the magnetic sources

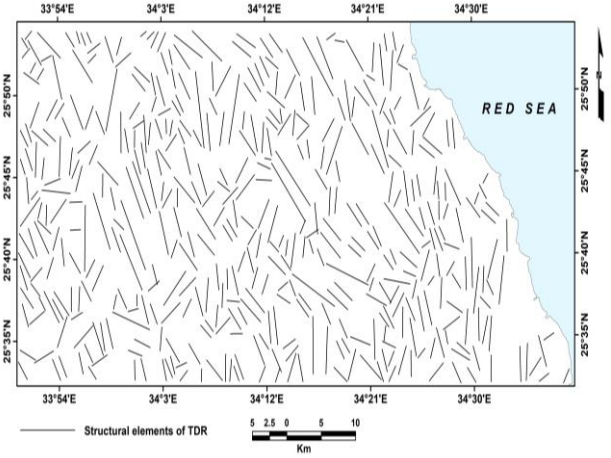

Figure 13: Interpreted structural map based on tilt derivative technique.

3.2.6. Euler deconvolution method (ED)

This method, proposed by Thompson (1982) [48], has become more widely used to measure the magnetic source location. The Euler's technique has been enhanced by Mushayandebvu et al. (2001) [49] to produce a more complete analysis of source parameters that permits the calculation of the dip and the susceptibility contrast. In this context, the euler deconvolution system selects a structural index that ranges from 0 to 3, to indicate the field's rate of change that depends on the geometry of the source. The structural index (SI) chosen affects the accuracy of depth measurement. Using the Euler method and a structural index of N = 1, the anomaly depths were computed (Fig. 14). The euler depth map of the study area clearly shows the basement depth ranges from <50 to >1000 m.

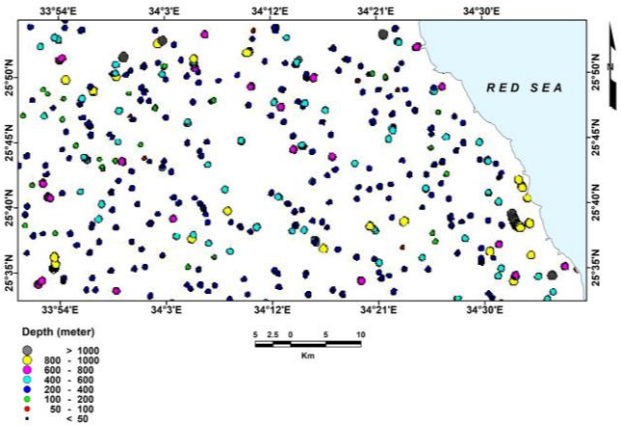

Figure 14: Euler deconvolution map of the area

3.3. Structural orientations

As previously mentioned, the study area covered by basement rocks (igneous and metamorphic) and sedimentary rocks. A number of geologic structures with different types, trends, and locations affected these rocks. The orientations of the structural are a reflection of the tectonic events that built them. An automated method using RockWorks17 program is used to extract the lineament directions. To define lineament direction, rose diagrams are made for each map of surface and sub surface structural elements.

The findings indicate that the area of study has been exposed to the surface and subsurface structural with varying trends as reported in figure 15 and table1. These structure lineaments have trends include NNW-SSE (Gulf of Suez trend), N-S (East African trend), and NE-SW (Gulf of Aqaba trend). Additionally, The NNW-SSE trend, which is extracted from the surface and subsurface with the highest present of length in compared with other trends, is the dominant structural trend in the region.

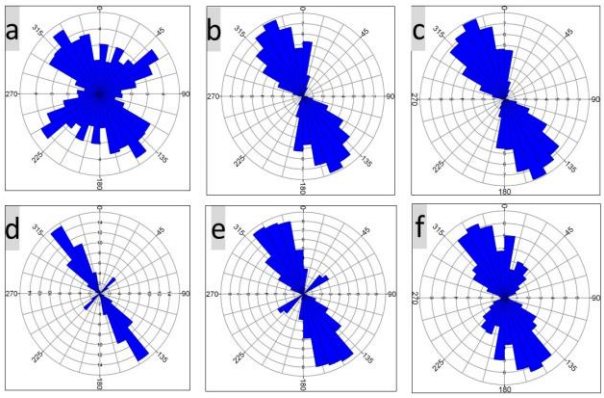

Fig.15: illustrate the orientations of lineaments traced from the (a) Geologic field map, (b), SRTM 30m DEM. (c) ALOS/PALSAR 12.5 DEM, (d) Reginal magnetic component (d) Residual magnetic component, and (f) Tilt derivative technique.

Table 1: Recorded the length percentage of extracted lineaments in the study area.

Method		Trend%		
		N-S	NNW SSE	NE-SW
Geology	Geologic map	28.6	39.2	32.2
Remote sensing	30m-DEM	46.2	53.8	….
	AlOS/PALSAR	43.5	56.5	….
Aero-magnetic	Regional	…	65.2	34.8
	Residual	30.1	45.5	24.4
	TDR	35.8	41.1	23.1

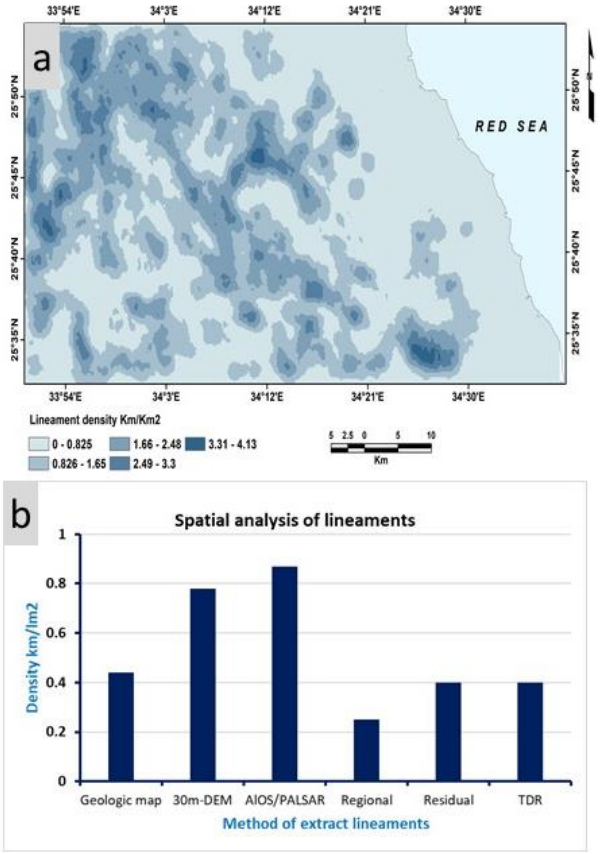

Fig. 16: a) Lineaments density map deduced from AlOS/PALSAR DEM as a selective example, b) Spatial analysis of the lineaments.

On the otherwise, the spatial distribution of structure lineaments derived by different methods is an effective tool for understanding the tectonic nature of the region. The GIS is a suitable environment for this analysis. Figure 16a displays a selective example to the spatial distribution of the lineaments traced from AlOS/PALSAR DEM. The lineaments density ranges from 0 to 4.13 km/km^2. Other analyzes are provided in the Appendix, table 2, and figure 16b. The results indicate that the lineaments extracted from the regional magnetic map (deep sources) are the lowest density, while the lineaments derived from remote sensing data

(surface sources) are the highest density. This may suggest that the density of the structures decreases with depth. On the other side, this may support that the term "lineaments" is more general in comparison to "faults" and "fracturs." in structure geology.

In this context, remote sensing data provide measurements with different resolutions to trace the surface lineaments. According to the findings, the two types of measurements, which have spatial resolutions of 12.5 and 30 metres, reported the same lineament trends. With regard to magnetic measurements, a number of techniques were used to accurately trace shallower and deeper structures. The findings showed that there is an important relationship between magnetic measurements and remote sensing data when extracting structure elements. In this regard, the surface structure in the research region reflect the presence of subsurface features. So, it's important to utilise remote sensing technology to make an initial decision before performing field investigations.

Table 2: Recorded the spatial distribution of the extracted lineaments in the study area.

Method		**Spatial distribution Km/km2**			
		Min.	Max.	Mean	SD
Geology	Geologic map	0	1.66	0.44	0.30
Remote sensing	30m-DEM	0	3.15	0.78	0.69
	AlOS/PALSAR	0	4.13	0.87	0.80
Aero-magnetic	Regional	0	1.20	0.25	0.26
	Residual	0	1.26	0.40	0.29
	TDR	0	1.40	0.40	0.29
Min; minimum		Mean; average			
Max; maximum		SD; standard deviation			

4. Conclusions

This paper deals with the mapping of the surface and subsurface structure of Gabal El-Syibaì Area, Central Eastern Desert, Egypt, from remote sensing and aeromagnetic measurements. The remote sensing technique represented in the SRTM 30m and AlOS/PALSAR DEM 12.5 m helped in extracting the surface lineaments of the study area. The DEM was re-projected to the metric system and subject to some corrections, then the shaded model was derived from it. DEM derived SRTM and DEM derived ALOS PALSAR reported the same lineament trends. In this regard, Aeromagnetic data was used to find subsurface lineaments. The magnetic measurements were corrected, and the outcome RTP data helped in deriving the structure lineaments. Through power spectral analysis, the residual and regional magnetic anomalies were extracted from RTP anomaly map. According to findings, the measured mean depths of deep and shallow causative body are, respectively, 1100 m and 400 m. Through the analysis of shallow-seated and deep-seated structural element maps, the study revealed the presence of three significant structural trends in the area under investigation.

The findings indicate that the area of study has been exposed to the surface and subsurface structural with varying length and intensity. The highest structure length was extracted from the deep sources, while the highest lineament density was deduced at the surface. These structures have trends include NNW-SSE (Gulf of Suez trend), N-S (East African trend), and NE-SW (Gulf of Aqaba trend). Although SRTM DEM and PALSAR DEM have different spatial resolutions of 12.5 and 30 metres, they report the same lineament trends. In this regard, there is an important relationship between magnetic measurements and remote sensing data when extracting structure elements. The surface structure in the research region reflect the presence of subsurface features. Additionally, the lineaments decrease in frequency with depth. These structures should be viewed from the point of view of environmental geohazard and mining prospecting.

References

1. Colwell, R. N. (1983). Manual of Remote Sensing American Society of Photogrammetry. Falls Church, Virginia.
2. Milbury, C. A., Smrekar, S. E., Raymond, C. A., & Schubert, G. (2007). Lithospheric structure in the eastern region of Mars' dichotomy boundary. Planetary and Space Science, *55*(3), 280-288.
3. Austin, J. R., & Blenkinsop, T. G. (2008). The Cloncurry Lineament: Geophysical and geological evidence for a deep crustal structure in the Eastern Succession of the

Mount Isa Inlier. Precambrian Research, **163**(1-2), 50-68.
4. Hussin, H., bt Fauzi, N., Jamaluddin, T. A., & Arifin, M. H. (2017). Rock Mass Quality Effected by Lineament Using Rock Mass Rating (RMR)–Case Study from Former Quarry Site. Earth Sciences Malaysia (ESMY), **1(2),** 13-16.
5. Kamp, U., Growley, B. J., Khattak, G. A., & Owen, L. A. (2008). GIS-based landslide susceptibility mapping for the 2005 Kashmir earthquake region. Geomorphology, **101(4),** 631-642.
6. Khan, H., Shafique, M., Khan, M. A., Bacha, M. A., Shah, S. U., & Calligaris, C. (2019). Landslide susceptibility assessment using Frequency Ratio, a case study of northern Pakistan. *The Egyptian Journal of Remote Sensing and Space Science*, ***22*(1),** 11-24.
7. Ladas I, Fountoulis I, & Mariolakos I. (2007). Using GIS and multicriteria decision analysis in landslide susceptibility mapping-a case study in Messinia prefecture area (SW Peloponnesus, Greece). Bulletin of the Geological Society of Greece, International Congress, Athens, **40(4)**, 1973-1985.
8. Sibson, R. H. (1986a). Earthquakes and lineament infrastructure. Philosophical Transactions of the Royal Society of London. Series A, Mathematical and Physical Sciences, **317**(1539), 63-79.
9. Sibson, R. H. (1986b). Brecciation processes in fault zones: inferences from earthquake rupturing. Pure and Applied Geophysics, **124,** 159-175.
10. Boucher, R. K. (1995). The relevance of lineament tectonics to hydrocarbon occurrences in the Cooper and Eromanga Basins, South Australia.
11. Rowan, L. C., & Bowers, T. L. (1995). Analysis of linear features mapped in landsat thematic mapper and sidelooking aitbome radar lmages of the reno L" by 2^{o} Quadrangle, Nevada and Califomia: lmplications fot mineral resource studies. Photogrammetric Engineering and remote sensing, **61(6),** 749-759.
12. Rowland, J. V., & Sibson, R. H. (2004). Structural controls on hydrothermal flow in a segmented rift system, Taupo Volcanic Zone, New Zealand. Geofluids, ***4*(4),** 259-283.
13. Masoud, A., Koike, K., & Teng, Y. (2007). Geothermal reservoir characterization integrating spatial GIS models of temperature, geology, and fractures. In Proc. 12th Conference of International Association for Mathematical Geology, Beijing, China, August (pp. 26-31).
14. Mineral Resources Authority (Geological Survey) (2014). Mineral Resources in the Arab Republic of Egypt – Ores for Mines, Quarries and Salines - 421 pages.
15. Conoco (1987). Egyptian general petroleum corporation-Conoco coral, 1987. Geological map of Egypt, Scale 1:500,000, Cairo.
16. Said, R. (1990). The geology of Egypt. Routledge.
17. EL-Bayoumi, R. A., & Greiling, R. (1984). Tectonic evolution of a Pan-African plate margin in Southeastern Egypt—a suture zone overprinted by low angle thrusting. In *Géologie africaine* (pp. 47-56).
18. El-Gaby, S., List, F. K., & Tehrani, R. (1988). Geology, evolution and metallogenesis of the Pan-African belt in Egypt. In the Pan-African belt of Northeast Africa and adjacent areas: tectonic evolution and economic aspects of a late proterozoic oregon (pp. 17-68).
19. Hassan, M. A., & Hashad, A. H. (1990). Precambrian of Egypt. The anorogenic alkalic rocks, Annal Geological Survery **9,** Egypt, 81-101.
20. Assran, H. M. (2005). Geology and structural synthesis of pan-african rocks, gabal el sibai area, central eastern desert, *egypt. Delta Journal of Science*, **29(2),** 117-135.
21. Fowler, A. R., Khamees, H., & Dowidar, H. (2007). El Sibai gneissic complex, Central Eastern Desert, Egypt: folded nappes and syn-kinematic gneissic granitoid sheets–not a core complex. *Journal of African Earth Sciences*, **49(4-5),** 119-135.
22. Sultan, M., Arvidson, R. E., Duncan, I. J., Stern, R. J., & El Kaliouby, B. (1988).

Extension of the Najd shear system from Saudi Arabia to the central Eastern Desert of Egypt based on integrated field and Landsat observations. Tectonics, **7(6),** 1291-1306.
23. Forkuor, G., & Maathuis, B. (2012). Comparison of SRTM and ASTER derived digital elevation models over two regions in Ghana-Implications for hydrological and environmental modeling (pp. 219-240). London: INTECH Open Access Publisher.
24. Patel, A., Katiyar, S. K., & Prasad, V. (2016). Performances evaluation of different open source DEM using Differential Global Positioning System (DGPS). *The Egyptian Journal of Remote Sensing and Space Science*, **19(1),** 7-16.
25. McCauley, J. F., Schaber, G. G., Breed, C. S., Grolier, M. J., Haynes, C. V., Issawi, B., & Blom, R. (1982). Subsurface valleys and geoarcheology of the eastern Sahara revealed by shuttle radar. Science, **218(4576)**, 1004-1020.
26. Aero Service. (1984). Aero Service Division of the Western Geophysical Company of America. The total magnetic intensity map of Egypt. The scale of 1: 50, 000.
27. Jordan, G., Meijninger, B. M. L., Van Hinsbergen, D. J. J., Meulenkamp, J. E., & Van Dijk, P. M. (2005). Extraction of morphotectonic features from DEMs: Development and applications for study areas in Hungary and NW Greece. *International journal of applied earth observation and geoinformation*, **7(3),** 163-182.
28. Zoheir, B., & Emam, A. (2014). Field and ASTER imagery data for the setting of gold mineralization in Western Allaqi–Heiani belt, Egypt: A case study from the Haimur deposit. *Journal of African Earth Sciences*, ***99***, 150-164.
29. Abdullah, A., Akhir, J. M., & Abdullah, I. (2010). Automatic mapping of lineaments using shaded relief images derived from digital elevation model (DEMs) in the Maran-Sungi Lembing area, Malaysia. *Electronic Journal of Geotechnical Engineering*, **15(6),** 949-958.
30. PCI Geomatica (2016). Remote sensing desktop software package. Users' Manual, Canada Center of Remote Sensing, Canada. http://www.pcigeomatics.com
31. Abdullah, A., Nassr, S., & Ghaleeb, A. (2013). Landsat ETM-7 for lineament mapping using automatic extraction technique in the SW part of Taiz Area, Yemen. *Global Journal of Human-Social Science Research*, ***13*(3),** 34-38.
32. Luo, Y., XUE, D. J., & Wang, M. (2010). Reduction to the pole at the geomagnetic equator. *Chinese Journal of Geophysics*, ***53*(6),** 1082-1089.
33. Ravat, D. (2007). Reduction to Pole. *Encyclopedia of Geomagnetism and Paleomagnetism. Switzerland: Springer*, 856-857.
34. Spector, A., & Grant, F. S. (1985). Statistical models for interpreting aeromagnetic data. Geophysics, **35(2),** 293-302.
35. Bhattacharyya, B. K. (1965). Two-dimensional harmonic analysis as a tool for magnetic interpretation. Geophysics, **30(5),** 829-857.
36. Hahn, A., Kind, E. G., & Mishra, D. C. (1976). Depth estimation of magnetic sources by means of Fourier amplitude spectra. Geophysical Prospecting, **24(2),** 287-306.
37. Abdallatif, T. F., & Lee, J. M. (2001). Shallow magnetic survey of the Younghae Basin area, South Korea: Evaluation of structural setting. *Geosciences Journal*, ***5*,** 327-338.
38. Al-Badani, M. A., & Al-Wathaf, Y. M. (2018). Using the aeromagnetic data for mapping the basement depth and contact locations, at southern part of Tihamah region, western Yemen. *Egyptian Journal of Petroleum*, ***27*(4),** 485-495.
39. Phillips, J. D. (2000). Locating magnetic contacts: a comparison of the horizontal gradient, analytic signal, and local wavenumber methods. In SEG Technical Program Expanded Abstracts 2000 (pp. 402-405). Society of Exploration Geophysicists.
40. Ibraheem, I. M. (2005). Structural studies on the northern part of Sinai using the potential field methods (Doctoral

dissertation, MSc. thesis, Ain Shams University, Cairo, Egypt).
41. Reford, M. S., & Sumner, J. S. (1964). Aeromagnetics. Geophysics, ***29*****(4),** 482-516.
42. Geosoft Program Oasis Montaj (2010**):** Geosoft Mapping and Processing System. (Geosoft Inc., Toronto, Canada. Scientific Research Publishing An Academic Publisher Copyright 2006-2017 Scientific Research Publishing Inc.
43. Dobrin, M. B., & Savit, C. H. (1960). Introduction to geophysical prospecting (Vol. **4**). New York: McGraw-hill.
44. Clarke, G. K. (1969). Optimum second-derivative and downward-continuation filters. Geophysics, **34(3),** 424-437.
45. Henderson, R. G., & Zietz, I. (1949). The computation of second vertical derivatives of geomagnetic fields. Geophysics, **14(4),** 508-516.
46. Miller, H. G., & Singh, V. (1994). Potential field tilt—a new concept for location of potential field sources. *Journal of applied Geophysics*, ***32*****(2-3),** 213-217.
47. Verduzco, B., Fairhead, J. D., Green, C. M., & MacKenzie, C. (2004). New insights into magnetic derivatives for structural mapping. The leading edge, ***23*****(2),** 116-119.
48. Thompson, D. T. (1982). EULDPH: A new technique for making computer-assisted depth estimates from magnetic data. Geophysics, **47(1),** 31-37.
49. Barbosa, V. C., Silva, J. B., & Medeiros, W. E. (1999). Stability analysis and improvement of structural index estimation in Euler deconvolution. Geophysics, **64(1),** 48-60.